

2022

3D Localization of Vena Contracta using Doppler ICE Imaging in Tricuspid Valve Interventions

Hareem Nisar
Western University, hnisar3@uwo.ca

Djalal Fakim
Western University

Daniel Bainbridge
LHSC

Elvis C.S. Chen
Western University

Terry M Peters
Imaging Research Laboratories, Robarts Research Institute, London, Ontario, Canada & Biomedical Engineering Graduate Program, Western University, London, Ontario, Canada & Department of Medical Biophysics, Western University, London, Ontario, Canada

Follow this and additional works at: <https://ir.lib.uwo.ca/robartspub>

Citation of this paper:

Nisar, Hareem; Fakim, Djalal; Bainbridge, Daniel; Chen, Elvis C.S.; and Peters, Terry M, "3D Localization of Vena Contracta using Doppler ICE Imaging in Tricuspid Valve Interventions" (2022). *Robarts Imaging Publications*. 28.

<https://ir.lib.uwo.ca/robartspub/28>

3D Localization of Vena Contracta using Doppler ICE Imaging in Tricuspid Valve Interventions

Hareem Nisar^{1,2*}, Djalal Fakim³, Daniel Bainbridge⁴, Elvis
C.S. Chen^{1,2,3,5} and Terry Peters^{1,2,3,5}

^{1*}Robarts Research Institute, , 1151 Richmond St., London,
N6A5B7, ON, Canada.

²School of Biomedical Engineering, Western University, 1151
Richmond St., London, N6A3K7, ON, Canada.

³Schulic School of Medicine and Dentistry, Western University,
1151 Richmond St., London, N6A3K7, ON, Canada.

⁴Department of Anesthesia and Perioperative Medicine, London
Health Sciences Centre, 339 Windermere Rd., London, N6A5A5,
ON, Canada.

⁵Department of Medical Biophysics, Western University, 1151
Richmond St., London, N6A3K7, ON, Canada.

*Corresponding author(s). E-mail(s): hnisar3@uwo.ca;

Contributing authors: dfakim2023@meds.uwo.ca;

daniel.bainbridge@lhsc.on.ca; chene@robarts.ca;

tpeters@robarts.ca;

Abstract

Purpose: Tricuspid valve (TV) interventions face the challenge of imag-
ing the anatomy and tools because of the ‘TEE-unfriendly’ nature of
the TV. TriClip device (Abbott Vascular, Canada) is used to repair
the leaflets to reduce the regurgitant blood flow in the TV, and a core
step during the deployment of the TriClip is to position the device per-
pendicular to the coaptation gap causing the regurgitation. In Doppler

001
002
003
004
005
006
007
008
009
010
011
012
013
014
015
016
017
018
019
020
021
022
023
024
025
026
027
028
029
030
031
032
033
034
035
036
037
038
039
040
041
042
043
044
045
046

047 ultrasound imaging, the coaptation gap corresponds to the neck of the
048 regurgitant jet called vena contracta (VC). In this study, we provide
049 a semi-automated method to localize the VC from Doppler intracardiac
050 echo (ICE) imaging in a tracked 3D space, thus providing a
051 pre-mapped location of the coaptation gap to assist device position-
052 ing. **Methods:** A magnetically-tracked ICE probe with Doppler imaging
053 capabilities is employed in this study for imaging three patient-specific
054 TVs placed in a pulsatile heart phantom. For each of the valves, the
055 ICE probe is positioned to image the maximum regurgitant flow for five
056 cardiac cycles. An algorithm then extracts the regurgitation imaging
057 and computes the exact location of the vena contracta on the image.
058 **Results:** Across the three pathological, patient-specific,
059 valves the average distance error between the detected
060 VC and the ground truth model is (1.22 ± 2.00) mm.
061 **Conclusion:** This study presented a method for ultrasound-
062 based localization of vena contracta in 3D space. Mapping
063 such anatomical landmarks has the potential to assist with
064 device positioning and to simplify tricuspid valve interventions.

065 **Keywords:** Tricuspid valve, cardiac interventions, intracardiac
066 echocardiography (ICE), image guided systems, vena contracta localization

070 1 Introduction

071
072 Previously labeled as the forgotten valve, the tricuspid valve (TV) and its
073 repair surgeries have gained prominence recently [1–3]. For the longest time, it
074 was believed that “the TV is designed to be(come) incompetent” [4] and that
075 the valve will heal itself after a left-sided surgery is performed [5]. Research and
076 experience have shown otherwise. When left untreated, even after mitral valve
077 surgery, the TV can develop high-grade regurgitation disease [6, 7]. Tricuspid
078 valve regurgitation (TR) is the most common valvular disease in the right side
079 of the heart, characterized by the backflow of blood from the right ventricle to
080 the right atrium, and can be organic or functional in nature. Around 80% of
081 the TR cases are functional and due to annulus dilation (diameter greater than
082 40 mm) and leaflet tethering caused by pressure overload [8]. The disease can
083
084
085
086
087
088
089
090
091
092

vary in severity, which in turn dictates the type of surgical intervention performed on the patient. Tricuspid repair is preferred over replacement surgeries as the replacement interventions are associated with a high mortality rate [3]. It is also suggested that the TV repair can be safely performed simultaneously with a mitral valve repair intervention [9].

Currently, there are several devices and procedures approved for tricuspid valve repair. These repair techniques can be classified into two major categories – annuloplasty and coaptation devices. The ring annuloplasty, such as Cardioband (Edwards Lifesciences), is recommended in patients with early-stage TR. The leaflet repair is performed as a more generic procedure, and on a variety of TV anatomical configurations [10]. The common devices deployed for coaptation enhancement of TV include the Forma Spacer (Edwards Lifesciences), the TriCinch (4Tech Cardio), and edge-to-edge repair devices like the MitraClip (Abbott Vascular), TriClip (Abbott Vascular) and Pascal (Edwards Lifesciences) [11]. These edge-to-edge repair techniques are particularly successful in treating severe TR with the benefits of reducing the need for hospitalization as a result of heart failure [12].

Earlier success in TV repair include the use of the MitraClip on the TV to reduce the regurgitation by at least one grade [13, 14]. Since then, a specialized tool called TriClip (Abbott Vascular, Santa Clara, California) was developed for the edge-to-edge repair of the tricuspid valve. The TriClip has proven itself to be a safe and effective device for TV repair via the TRILUMINATE trial [15]. In 2020, the TriClip received approval for a CE mark.

The leaflet repair via the TriClip is performed percutaneously via transfemoral access and while a transjugular approach has also been developed, the transfemoral approach has shown superior performance [16]. The clip is deployed either using the triple-orifice technique or more commonly, using a

139 bicuspidization method. In this latter technique, the clip is placed between the
140 anterior and septal leaflets of the TV to achieve the best post-procedural out-
141 comes [17]. Currently, this procedure is performed under general anesthesia
142 and the combined fluoroscopic and transesophageal echocardiographic (TEE)
143 imaging. The tools are inserted into the right atrium and maneuvered carefully
144 and iteratively using control knobs, fasteners, and levers to reach the TV in
145 the right ventricle under image guidance [16]. Lebehn et al. describe a protocol
146 for TEE imaging during these various steps involved in the device position-
147 ing [18], where device positioning involves localizing the leaflet coaptation gap
148 at the leaflet tips and the assessment of the regurgitation based on the vena
149 contracta. This is followed by the positioning of clip arms perpendicular to the
150 coaptation gap.

151
152
153
154
155
156
157
158
159 Positioning the TriClip at the coaptation gap is one of the most critical
160 steps during a TV repair intervention. When describing the device position-
161 ing process, Nickenig et al. mention that “the catheter tip was manipulated
162 (via the control knobs on the handles) in the right atrium until the clip was
163 properly oriented perpendicular to the line of coaptation of the tricuspid valve
164 leaflets” [15]. This step is similar to the mitral valve repair interventions where
165 a closed clip is advanced to the site of the regurgitant jet under TEE guid-
166 ance [19]. Device positioning using these steps is an established procedure for
167 left-sided interventions, however, the same task becomes much more meticu-
168 lous for right-sided cardiac interventions due to the constraint nature of the
169 TEE.

170
171
172
173
174
175
176
177 The tricuspid valve and its interventions have been declared “TEE-
178 unfriendly”. The TV is located anterior to the mitral valve, rendering it
179 challenging to image using a TEE probe [20]. The large distance between
180 the TEE probe and the TV, combined with the non-perpendicular alignment
181
182
183
184

of the sub-valvular apparatus also makes the TEE imaging of the TV more demanding [21]. Quite often, the acquired TEE images of the TV are of sub-optimal quality due to the presence of shadowing and complex TV anatomy. In such cases, it is recommended to introduce intracardiac echocardiography (ICE) into the procedural imaging [16]. ICE imaging can not only aid in the imaging of leaflets and tricuspid annulus but also guide the deployment of the tool correctly.

ICE ultrasound provides high-resolution imaging of cardiac structures. with several advantages over conventional TEE imaging. ICE imaging of the TV allows the anatomy to be viewed up close and provides clear and direct imaging of the sub-valvular apparatus. Unlike TEE, the insertion of an ICE probe can be performed under local anesthesia only and without the need for specialized operator. ICE is also well tolerated by the patients. The major drawback of this technology is the high cost of each single-use probe, but it has the potential to offer a better cost/benefit ratio, by reducing the procedure times and length of post-op hospitalization in patients. ICE has made its mark in interventional cardiology for structural heart diseases and electrophysiology [22, 23]. Enriquez et al. have provided a detailed review of the current use of ICE in cardiology [24]. ICE has also been a favorable choice for the interventional imaging of the tricuspid valve, where it may be utilized for discerning the annulus from the leaflets, and for guiding tool positioning and orientation [25]. In several studies, ICE is used in conjunction with fluoroscopy or TEE to guide the tools and repair the TV in both annuloplasty and edge-to-edge repair [26–30].

Image-guided systems (IGS) have helped simplify many interventions, as well as having made them safer and more reproducible [31]. In a meta-analysis comparing the efficacy of image-guided and standard cardiac resynchronization therapy in patients with heart failure, Jin et al. demonstrated that a strategy

231 of echocardiographic guidance was associated with improved outcomes com-
232 pared with a routine strategy [32]. IGS can greatly benefit TAVI procedure
233 in patients with complex and unusual anatomy, such as bicuspid aortic steno-
234 sis and situs inversus totalis [33]. As the push towards less-invasive cardiac
235 therapies continues, image-guided intracardiac visualization has received clin-
236 ical exposure, as it has the potential to improve the precision and outcome of
237 surgical procedures [31].
238

242 To facilitate the positioning of a TriClip device, the identification and local-
243 ization of coaptation gap is a crucial step, that can potentially be simplified by
244 pre-mapping the 3D location of the coaptation gap prior to the device being
245 positioned. This mapped location serves as an important landmark during the
246 TriClip positioning stage. In ultrasound imaging, the neck of the regurgitant
247 jet, as seen in the color Doppler, is called the vena contracta (VC) and it cor-
248 responds to the location of the coaptation gap. In this study we aim to map
249 the coaptation gap by localizing the vena contracta in Doppler ICE imaging.
250

256 While there is currently no commercially available automatic VC and annu-
257 lus detection system, several automatic VC quantification techniques have been
258 published in the past for the assessment of mitral regurgitation using TEE [34]
259 and TTE [35]. Sotaquira et al. have developed an algorithm to automatically
260 detect and quantify the shape of the effective regurgitant orifice area using 3D
261 TEE [36], and Li et al. have developed a rapid MVA tracking algorithm for use
262 in the guidance of off-pump beating heart transapical mitral valve repair using
263 2D biplane TEE images [37]. The eventual goal of these developments is the
264 creation of an image-guided system (IGS) for cardiac interventions in order to
265 provide more timely and accurate information to the interventionalists.
266

272 To summarize the clinical need - TV repair interventions are challeng-
273 ing due to the anatomical complexity and lack of standard, reliable imaging
274

protocols. A crucial step during these procedures is to align the device perpendicular to the coaptation gap or the site of the regurgitation. This step, along with others during the device positioning stage, is currently performed using suboptimal TEE imaging. ICE has been a suitable choice for imaging the tricuspid valve and its subapparatus as it allows one to view the tricuspid anatomy directly. ICE imaging, when used with an image-guidance system, holds the potential to provide more contextual information and facilitate the device positioning during edge-to-edge transcatheter TV repair interventions.

In order to assist the positioning of coaptation device at the site of regurgitation, we propose to use a tracked ICE probe with Doppler imaging. An ICE probe can simplify this procedural step by identifying the site of regurgitation i.e. vena contracta from ultrasound images, and representing its location in 3D space. Tracked devices can then navigate to reach the targeted vena contracta. To the best of our knowledge, this paper presents the first image-guidance system for tricuspid valve interventions. A proof of concept study, performed on a simple silicone wall phantom, has been conducted by our lab and accepted for publication at the SPIE 2022 conference. In this paper, we present a guidance system which uses ICE imaging and EM tracking technology to identify the site of regurgitation from a patient-specific tricuspid valve in a beating heart phantom. This system is developed on 3DSlicer and implemented as an open-source, one-click, 3DSlicer module. The module, as well as some test data along with a video demonstration, can be found at <https://github.com/hareem-nisar/VC-localization>.

277
278
279
280
281
282
283
284
285
286
287
288
289
290
291
292
293
294
295
296
297
298
299
300
301
302
303
304
305
306
307
308
309
310
311
312
313
314
315
316
317
318
319
320
321
322

2 Materials and Methods

2.1 Materials

In this study, we used a 10-French, forward-looking, and radial Foresight™ ICE probe along with the Hummingbird Console (Conavi Medical Inc., Toronto, Canada) to acquire ultrasound imaging of the valve. The Foresight™ ICE is unique as it provides radial ultrasound as well as Doppler imaging capabilities [38], thus enabling the direct visualization of the anatomy and the regurgitation during interventions.

To achieve magnetic tracking (MT) of the ultrasound, we utilized the Aurora Tabletop Field Generator (NDI, Waterloo, Canada) and a 6 DoF sensor to track the ICE probe in 3D space during data collection.

LV Plus Simulator (Archetype Biomedical Inc., London, Canada) was used as a pulsatile heart phantom to simulate a ventricle and an atrial chamber. The phantom can be equipped with patient-specific valves, which includes the valve leaflets embedded in a silicone flange for support[39]. The details of the methods used in the modelling of TV are given in the next section. Three patient-specific valves are created using this technique.

2.2 TV modeling procedure

The negative mold of a silicone flange (11 cm in diameter, 3 mm thick) with patient modeled tricuspid valves [39] was created using an Ultimaker S5 3D Printer (Ultimaker, Utrecht, Netherlands) and printed using ToughPLA filament. Approximately 3 cm of the ends of 30 cm of dacron string were frayed to mimic chordae tendineae. A 50:50 by weight mixture of previously degassed (-0.8 atm at 1 min) Part A and Part B of Mold Star™ Eco Flex-003 was brushed on the TV valve mold leaflets. The Mold Star™ Eco Flex-003 was pigmented white with Silc-Pig Silicone Pigment to allow for easy visualization. The frayed

ends of the dacron string were carefully placed onto the leaflets, with each leaflet being attached to two dacron strings. Once the dacron cordae tendinae were securely positioned, the leaflets were coated once more with the Mold Star™ Eco Flex-003 mixture. The silicone leaflets were allowed to cure for 30 min. To make the silicone flange surrounding the valve, a 50:50 by weight mixture of previously degassed (-0.8 atm at 1 min) Part A and Part B of Mold Star™ Slow 15 was then poured into the mold. The silicone flange was allowed to cure at room temperature and pressure for 45 min prior to removal from the negative mold.

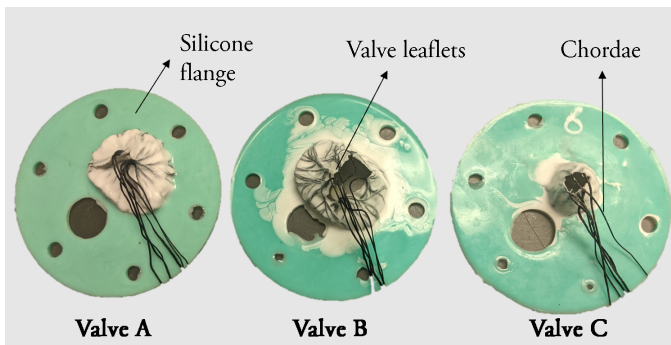


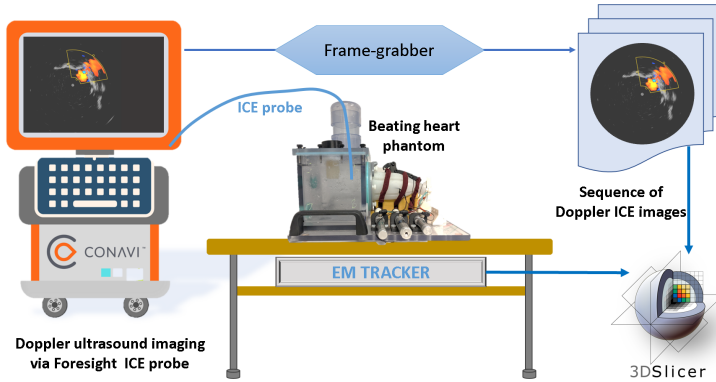
Fig. 1 Three patient specific tricuspid valves modeled using silicone and dacron strings.

2.3 Data Collection

An MT sensor was attached externally to a Foresight™ ICE probe using an adhesive. Prior to imaging, the ICE probe (in Doppler mode) was spatially calibrated using a point-to-line registration method [40, 41].

The pulsatile heart phantom was placed over the table-top MT field generator. The phantom was set to a normal rhythm at 60 beats per minute. Pure talc powder was used as an ultrasound contrast agent to enhance Doppler imaging. The ICE probe, in Doppler mode, was positioned in multiple locations at which a regurgitant jet could be observed. The regurgitation was produced

415 via the patient-specific, pathological tricuspid valves fitted inside the beating
 416 heart phantom. Three TVs (valves A, B, and C) were prepared and fitted
 417 heart phantom. Three TVs (valves A, B, and C) were prepared and fitted
 418 consecutively to acquire data. It must be noted that valve C was a pediatric,
 419 infant valve which was comparatively smaller than valves A and B.



435 **Fig. 2** Experimental setup - Ultrasound images are acquired using a frame grabber from
 436 the Conavi's Hummingbird console. A tracked ICE probe is positioned inside a beating heart
 437 phantom to image the patient-specific tricuspid valve. Image and tracking information is
 438 sent to a 3D Slicer module for processing.
 439

442 Images were acquired from the Hummingbird console display using a frame-
 443 grabber (Epiphan, Ottawa, Canada) at a rate of 15 frames/second. The data
 444 were recorded using the Plus Server to communicate ultrasound and track-
 445 ing information to 3D Slicer. For each of the three valves, five datasets were
 446 acquired, with each containing at least 5 seconds of imaging and tracking infor-
 447 mation. These data were processed to localize the vena contracta in 3D from
 448 the tracked, Doppler imaging of pathological tricuspid valves in real-time.
 449

455 2.4 Data Processing

457 The first step, to isolate the images with maximum regurgitation (Figure 3(a)),
 458 was performed semi-automatically by the user. The peak valvular regurgitation
 459
 460

usually occurs somewhere during the systolic phase of the cardiac cycle. To identify the exact phase of peak regurgitation, the user scans the first few images in a dataset to manually identify the first image exhibiting the highest regurgitation, along with the number of subsequent US images to be selected from each cardiac cycle. Then, all the images present at the selected cardiac phase were automatically isolated by our designed Slicer module using the data acquisition-rate information from the frame-grabber and the beating rate selected of the heart phantom. These images were stored in a ‘Sequence’ in 3D Slicer.

This sequence of peak-regurgitant Doppler ultrasound images was then processed to remove all the grayscale, B-mode information from all the images. Since the objective is to isolate the vena contracta, the non-regurgitant blood flow (depicted in cool colors) was also removed from the images by suppressing the pixels with blue channel information. It must be noted that the quality of regurgitant jet from individual cardiac cycles can sometimes be suboptimal. Therefore, to acquire an adequate jet image, all the images in the sequence were compounded together into one resultant image with the regurgitant flow (Figure 3(c)). This step was achieved by using the maximum intensity projection (MIP) principle. In doing so, the most yellow pixel or the highest velocity information is retained in the resultant image.

461
462
463
464
465
466
467
468
469
470
471
472
473
474
475
476
477
478
479
480
481
482
483
484
485
486
487
488
489
490
491
492
493
494
495
496
497
498
499
500
501
502
503
504
505
506

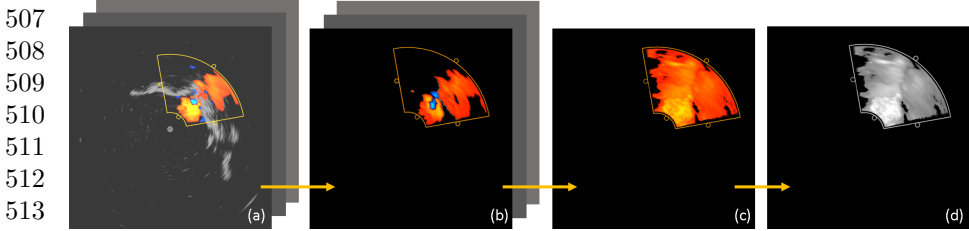


Fig. 3 (a) Sequence of Doppler ICE imaging with maximum regurgitant flow. (b) Imaging sequence containing Doppler information only undergoes maximum intensity projection to create (c) a resultant image with all the highest-velocity Doppler information. This resultant image is then converted to (d) a grayscale image for further processing.

The resultant combined Doppler image contained the complete regurgitant jet, depicting blood flowing backward from the ventricle to the atrial chamber (Figure 3(c)), and was converted to grayscale for further processing. The image was subjected to a binary threshold at an intensity of 150 to segment the brighter pixels representing the higher velocities in the regurgitant jet. For valve C, this threshold was set to 130 to accommodate the flow through a smaller, infant valve.

The next step was to identify the axis of the regurgitant jet. The segmented region was subjected to principal component analysis (PCA) to identify the major and minor axis of the jet, as well the principal moments. This information was used to transform the segmented region to lie along the major axis (Figure 4(b)). The noise was removed by retaining only the largest connected island within the segmented region which was representative of the atrial regurgitant jet.

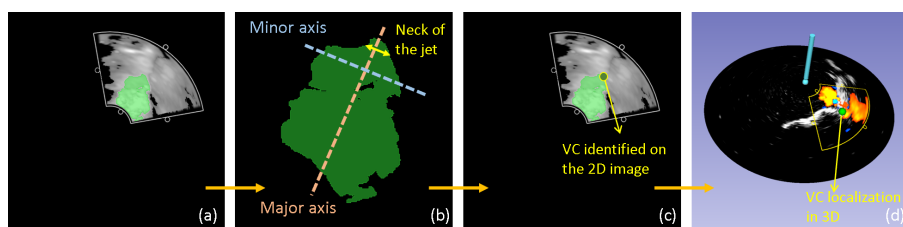


Fig. 4 (a) Resultant Doppler image overlaid with the segmentation of the regurgitant jet. (b) Principal component analysis of the segmented region to derive the location of the vena contracta (VC). VC localization seen on (c) a 2D image and in (d) 3D tracking space.

From the transformed regurgitant jet, our proposed algorithm then identified the location of the vena contracta. At each point along the major axis, the height of the segmentation was measured, and the point with the minimum height was recorded. This minimum height was estimated as the vena contracta width (VCW), while the midpoint along the VCW was noted as the transformed vena contracta location. The inverse transformation from the PCA was applied to retrieve the original coordinates for the location of vena contracta in the US image. Figure 4 shows the VCW on the segmented jet region and the vena contracta location placed on a 2D ICE image.

The ForesightTM ICE images are conical in nature, and lie in 3D space. The ICE image displayed on the console is a projection of the conical surface image along the height-axis. As such, the location of vena contracta on 2D images is not accurate and lacks the third dimension. Using the imaging angle information provided on the console screen, the location of the VC with respect to the true 3D image is calculated. The details of this conversion can be found in Nisar et al. [41]. Finally, the ICE probe calibration information, and the probe location transform, provided by the EM tracking system, were applied to acquire the location of the VC in 3D space (Figure 4(d)). This location

553
554
555
556
557
558
559
560
561
562
563
564
565
566
567
568
569
570
571
572
573
574
575
576
577
578
579
580
581
582
583
584
585
586
587
588
589
590
591
592
593
594
595
596
597
598

599 represents the origin of the regurgitation in the tricuspid valve, which occurs
600 most often at the coaptation gap.
601

602

603 **2.5 Validation**

604

605 Prior to data collection for each valve, the ground truth VC and annulus were
606 identified for validation. A pre-tracked and pre-calibrated needle was used
607 to identify the VC in 3D tracking space, where the tip of the needle, and
608 the orientation of the needle shaft, are tracked. The position of the ground
609 truth of the VC was obtained by visually identifying and manually tracing the
610 periphery of the regurgitant orifice using the tracked needle tip. The points
611 were used to construct a 3D model of the ground truth vena contracta (Figure
612 6). Similarly, the outline of the annulus points were marked, and the model was
613 constructed. The VC point locations detected by the algorithm were compared
614 to the manually isolated ground truth VC model by estimating the closest
615 distance between them.
616
617
618
619
620
621
622
623

624

625

626 **3 Results**

627

628 For each of the valves, the distance between the ground truth VC model and
629 the ICE-derived vena contracta locations were computed. The distance error
630 for all the datasets can be seen in Figure 5. As can be seen by the three tall
631 peaks in the graph, there is one outlier case for each valve where the error
632 is unacceptable. The outliers were a result of insufficient Doppler imaging as
633 captured by the framegrabber. Across the three valves and excluding the three
634 outliers, the average distance error between the detected VC and the ground
635 truth model is 1.22 ± 2 mm.
636
637
638
639

640

641

642

643

644

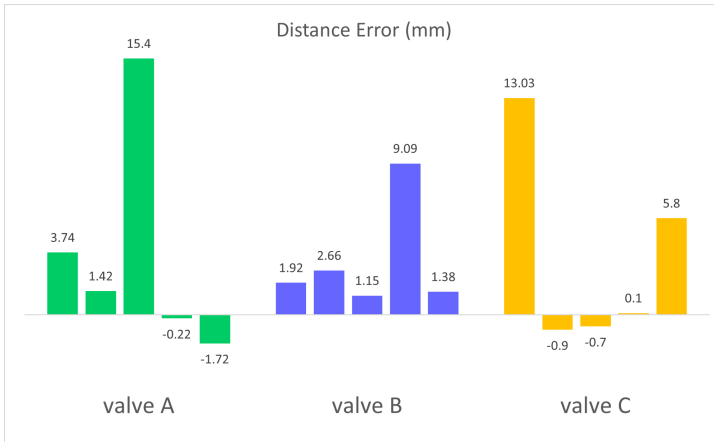


Fig. 5 Error bars representing the minimum distance between the algorithm-detected vena contracta location and the ground truth model. For each of the valves, one high error bar can be seen as an outlier.

Qualitatively, the position of the ground truth vena contracta, corresponding to the coaptation gap, can be seen as an irregular shaped body in yellow in Figure 6. The manually identified annulus ring is also represented to provide contextual information. The three high-error points can be seen near to the annulus in 3D which is a clear indication of these points as being incorrect and outliers. For valve A and B, the detected VC locations are close to the ground truth. The highest error was recorded in a dataset for valve C at 5.8mm.

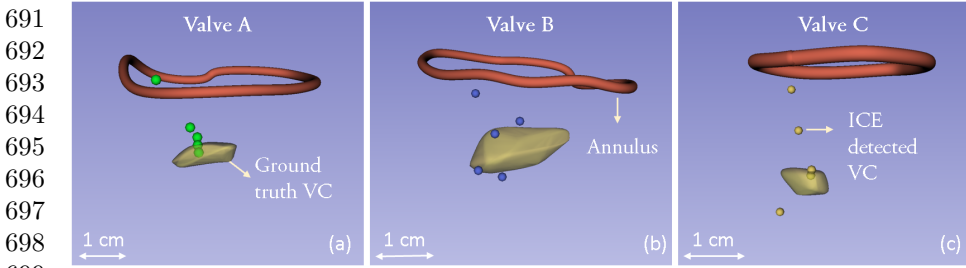


Fig. 6 A qualitative analysis of the results showing the ICE-derived vena contracta locations as points and the ground truth vena contracta as a model (in yellow). A pre-mapped annulus model and vena contracta location in a tracked environment can provide more contextual landmarks for device positioning

4 Discussion

During interventions, clinicians rely on anatomical landmarks to guide and align the tools properly. Traditionally the identification of landmarks and the positioning of tools takes place simultaneously, thus making the procedure intricate and demanding. Pre-mapping these landmarks can simplify these procedures by providing more information to the clinician while they position the devices. In this study, we present a method to semi-automatically extract the location of vena contracta, a clinically relevant landmark, from ultrasound images and represent it in 3D space. Results indicate that the designed 3D Slicer module can reliably localize the VC in most cases. Literature suggests that for cardiac interventions an error margin of up to 5 mm is acceptable [42]. In comparison, our average error of 1.22 ± 2 mm is appropriate for this early-stage study. It should also be noted that the ground truth established in these experiments should be considered as a "bronze" standard as it was manually identified by visual characterization of the coaptation gap. Hence it is susceptible to both human error and subjectivity.

A major limitation of this study is the presence of the outliers when the algorithm is unable to identify the VC accurately and instead the VC is localized near the annulus. In a use case, an outlier can be easily identified when the detected VC was positioned too close to the TV annulus. Outliers indicate that the valve should be reimaged and processed by the algorithm again. We suspect these outliers to be a result of the lower frame rate used in the study which meant that the regurgitation was not captured in the imaging data. During the experiments, it was observed that the recorded data in Slicer lacked some of the imaging frames showing high regurgitation on the Hummingbird console screen. The frame grabber was operating at a rate of 15 frames per second and in some cases missed capturing the image frame with the maximum regurgitation. To record the complete regurgitant Doppler imaging, we recommend using a frame grabber with a higher frame rate. Ideally, the imaging data should be transmitted directly from the ultrasound machine but this infrastructure is not yet available in most of the clinical console, including the Hummingbird console, used in this study.

A consideration while imaging the valve would be to use a narrower field of view for Doppler imaging to optimize and focus in the direction of the regurgitant jet. This simple factor can greatly enhance the overall efficiency of the designed algorithm.

Besides the VC, the annular ring of the tricuspid valve is another important landmark during TV interventions. In this study we manually identified the annulus ring, however, the procedures can benefit from automated ultrasound-based techniques to identify the TV annulus in 3D space. Future work can involve implementation of the existing methods in the literature that can extract and model the annulus from ultrasound. Li et al. [37] present a method

737
738
739
740
741
742
743
744
745
746
747
748
749
750
751
752
753
754
755
756
757
758
759
760
761
762
763
764
765
766
767
768
769
770
771
772
773
774
775
776
777
778
779
780
781
782

783 for tracking the mitral valve annulus and it can potentially be adapted for TV
784 annulus modeling as well.

786 Since the valves used in this study are modeled after real patient-specific
787 TV, there is room for collecting more and complex tricuspid regurgitation
788 cases. The valve modeling technique and the beating heart phantom allow
789 mimicking realistic conditions, reducing the need for in-vivo testing at such
790 an early stage of the study. With a variety of TV models, the algorithm can
791 be made more robust by testing and modifying it to accommodate more ver-
792 satile patient cases. Future work can involve making the Slicer module more
793 robust and suitable for even more complex tricuspid valve pathologies. The
794 ultrasound guidance approach can also be enhanced with the emerging 4D
795 ICE technology, like VeriSight Pro (Philips) and NuVision (Biosense Web-
796 ster), which provides improved imaging of the subvalvular apparatus during
797 transcatheter TV repair.

806

807 **5 Conclusion**

808

810 Tricuspid valve interventions and related technology are evolving as more cases
811 are being performed with imaging being a major challenge in them. A suitable
812 alternative to the existing TEE-based workflows is to employ ICE imaging
813 to visualize the anatomy. In this paper, we presented a method to provide
814 more contextual information to the interventionalists during the TV repair
815 procedures to reduce the regurgitation. A tracked ICE probe can be used to
816 localize and pre-map significant landmarks in order to assist the meticulous
817 task of device positioning during TV repair. Image guidance systems with
818 mapping technology have successfully simplified complex cardiac procedures
819 like ablation therapy [43]. This study is one step towards using image guidance

826

827

828

for tricuspid valve interventions to potentially streamline the challenging TV repair procedures. 829
830
831

Acknowledgments. The authors would like to thank John Moore for his valuable time and insights provided during this study. 832
833
834
835

Declarations 836

Funding 837

This study was funded by Canadian Foundation for Innovation (20994) and the Canadian Institutes for Health Research (FDN 201409). 838
839
840
841
842
843
844

Competing Interests 845

The authors have no relevant financial or non-financial interests to disclose. 846
847
848
849

Ethics approval 850

Not applicable 851
852
853
854
855

Consent to participate 856

Not applicable 857
858
859
860
861

Consent for publication 862

Not applicable 863
864
865
866
867

Availability of data and materials 868

The 3D Slicer module, test data, and a video demonstration can be found at <https://github.com/hareem-nisar/VC-localization>. 869
870
871
872
873
874

875 **Code availability**

876

877 Complete code is available at <https://github.com/hareem-nisar/VC->
878 localization.

880

881

882 **Authors' contributions**

883

884 All authors contributed to the study conception and design. Material prepara-
885 tion, data collection and analysis were performed by Hareem Nisar and Djalal
886 Fakim. The first draft of the manuscript was written by Hareem Nisar and all
887 authors commented on previous versions of the manuscript. All authors read
888 and approved the final manuscript.

891

892

893

894 **References**

895

896 [1] Enriquez-Sarano, M., Messika-Zeitoun, D., Topilsky, Y., Tribouilloy, C.,
897 Benfari, G., Michelena, H.: Tricuspid regurgitation is a public health crisis.
898 Progress in Cardiovascular Diseases **62**(6), 447–451 (2019). [https://doi.](https://doi.org/10.1016/j.pcad.2019.10.009)
899 [org/10.1016/j.pcad.2019.10.009](https://doi.org/10.1016/j.pcad.2019.10.009)

902

903

904 [2] Bouleti, C., Juliard, J.-M., Himbert, D., Iung, B., Brochet, E., Urena, M.,
905 Dilly, M.-P., Ou, P., Nataf, P., Vahanian, A.: Tricuspid valve and percuta-
906 neous approach: No longer the forgotten valve! Archives of Cardiovascular
907 Diseases **109**(1), 55–66 (2016). [https://doi.org/10.1016/J.ACVD.2015.08.](https://doi.org/10.1016/J.ACVD.2015.08.002)
908 [002](https://doi.org/10.1016/J.ACVD.2015.08.002)

911

912

913 [3] Zack, C.J., Fender, E.A., Chandrashekar, P., Reddy, Y.N.V., Bennett,
914 C.E., Stulak, J.M., Miller, V.M., Nishimura, R.A.: National Trends and
915 Outcomes in Isolated Tricuspid Valve Surgery. Journal of the American
916 College of Cardiology **70**(24), 2953–2960 (2017). [https://doi.org/10.1016/](https://doi.org/10.1016/J.JACC.2017.10.039)
917 [J.JACC.2017.10.039](https://doi.org/10.1016/J.JACC.2017.10.039)

920

- [4] Huttin, O., Voilliot, D., Mandry, D., Venner, C., Juillière, Y., Selton-Suty, C.: All you need to know about the tricuspid valve: Tricuspid valve imaging and tricuspid regurgitation analysis. *Archives of Cardiovascular Diseases* **109**(1), 67–80 (2016). <https://doi.org/10.1016/J.ACVD.2015.08.007>
- [5] Braunwald, N.S., Ross, J., Morrow, A.G.: Conservative management of tricuspid regurgitation in patients undergoing mitral valve replacement. *Circulation* **35**(4 Suppl), 63–9 (1967). <https://doi.org/10.1161/01.cir.35.4s1.i-63>
- [6] Antunes, M.J., Barlow, J.B.: Management of tricuspid valve regurgitation. *Heart* **93**(2), 271 (2007). <https://doi.org/10.1136/HRT.2006.095281>
- [7] Ancona, F., Stella, S., Taramasso, M., Marini, C., Latib, A., Denti, P., Grigioni, F., Enriquez-Sarano, M., Alfieri, O., Colombo, A., Maisano, F., Agricola, E.: Multimodality imaging of the tricuspid valve with implication for percutaneous repair approaches. *Heart* **103**, 1073–1081 (2017). <https://doi.org/10.1136/heartjnl-2016-310939>
- [8] Hansing, C.E., Rowe, G.G.: Tricuspid Insufficiency. *Circulation* **45**(4), 793–799 (1972). <https://doi.org/10.1161/01.CIR.45.4.793>
- [9] Hausleiter, J., Braun, D.: Mitral Meets Tricuspid: Is Severe Tricuspid Regurgitation a Bystander or Is There a Need for Combined Percutaneous Mitral and Tricuspid Valve Repair? *JACC: Cardiovascular Interventions* **11**(12), 1152–1153 (2018). <https://doi.org/10.1016/J.JCIN.2018.05.013>
- [10] Mangieri, A., Pagnesi, M., Regazzoli, D., Laricchia, A., Ho, E., Goldberg, Y., Chau, M., Gallo, F., Fiscaro, A., Khokhar, A., Colombo, A., Giannini,

- 967 F., Latib, A.: Future Perspectives in Percutaneous Treatment of Tricuspid
968 Regurgitation. *Frontiers in Cardiovascular Medicine* **7**, 581211 (2020).
969 <https://doi.org/10.3389/fcvm.2020.581211>
970
971
972
- [11] Goliasch, G., Mascherbauer, J.: Interventional treatment of tricuspid
973 regurgitation. *Wiener klinische Wochenschrift* 2020 132:3 **132**(3), 57–60
974 (2020). <https://doi.org/10.1007/S00508-020-01621-0>
975
976
977
- [12] Orban, M., Rommel, K.-P., Ho, E.C., Unterhuber, M., Pozzoli, A., Con-
978 nelly, K.A., Deseive, S., Besler, C., Ong, G., Braun, D., Edwards, J.,
979 Miura, M., Gülmez, G., Stolz, L., Gavazzoni, M., Zuber, M., Orban,
980 M., Nabauer, M., Maisano, F., Thiele, H., Massberg, S., Taramasso,
981 M., Fam, N.P., Lurz, P., Hausleiter, J.: Transcatheter Edge-to-Edge
982 Tricuspid Repair for Severe Tricuspid Regurgitation Reduces Hospital-
983 izations for Heart Failure. *JACC: Heart Failure* **8**(4), 265–276 (2020).
984 <https://doi.org/10.1016/j.jchf.2019.12.006>
985
986
987
988
989
990
991
992
- [13] Taramasso, M., Pozzoli, A., Guidotti, A., Nietlispach, F., Inderbitzin,
993 D.T., Benussi, S., Alfieri, O., Maisano, F.: Percutaneous tricuspid valve
994 therapies: the new frontier. *European Heart Journal*, 766 (2016). <https://doi.org/10.1093/eurheartj/ehv766>
995
996
997
998
999
- [14] Nickenig, G., Kowalski, M., Hausleiter, J., Braun, D., Schofer, J.,
1000 Yzeiraj, E., Rudolph, V., Friedrichs, K., Maisano, F., Taramasso, M.,
1001 Fam, N., Bianchi, G., Bedogni, F., Denti, P., Alfieri, O., Latib, A.,
1002 Colombo, A., Hammerstingl, C., Schueler, R.: Transcatheter Treatment of
1003 Severe Tricuspid Regurgitation With the Edge-to-Edge MitraClip Tech-
1004 nique. *Circulation* **135**(19), 1802–1814 (2017). [https://doi.org/10.1161/
1005 CIRCULATIONAHA.116.024848](https://doi.org/10.1161/CIRCULATIONAHA.116.024848)
1006
1007
1008
1009
1010
1011
1012

- [15] Nickenig, G., Weber, M., Lurz, P., von Bardeleben, R.S., Sitges, M., Sorajja, P., Hausleiter, J., Denti, P., Trochu, J.N., Nábauer, M., Dahou, A., Hahn, R.T.: Transcatheter edge-to-edge repair for reduction of tricuspid regurgitation: 6-month outcomes of the TRILUMINATE single-arm study. *The Lancet* **394**(10213), 2002–2011 (2019). [https://doi.org/10.1016/S0140-6736\(19\)32600-5](https://doi.org/10.1016/S0140-6736(19)32600-5)
- [16] Muntané-Carol, G., Alperi, A., Faroux, L., Bédard, E., Philippon, F., Rodés-Cabau, J.: Transcatheter Tricuspid Valve Intervention: Coaptation Devices. *Frontiers in Cardiovascular Medicine* **7**, 139 (2020). <https://doi.org/10.3389/FCVM.2020.00139>
- [17] Vismara, R., Gelpi, G., Prabhu, S., Romitelli, P., Troxler, L.G., Mangini, A., Romagnoni, C., Contino, M., Van Hoven, D.T., Lucherini, F., Jaworek, M., Redaelli, A., Fiore, G.B., Antona, C.: Transcatheter Edge-to-Edge Treatment of Functional Tricuspid Regurgitation in an Ex Vivo Pulsatile Heart Model. *Journal of the American College of Cardiology* **68**(10), 1024–1033 (2016). <https://doi.org/10.1016/j.jacc.2016.06.022>
- [18] Lebehn, M., Nikolou, E., Grapsa, J., Hahn, R.T.: Edge-to-Edge Tricuspid Valve Repair. *JACC: Case Reports* **2**(8), 1093–1096 (2020). <https://doi.org/10.1016/j.jaccas.2020.06.018>
- [19] Sherif, M.A., Paranskaya, L., Yuecel, S., Kische, S., Thiele, O., D’Ancona, G., Neuhausen-Abramkina, A., Ortak, J., Ince, H., Öner, A.: MitraClip step by step; how to simplify the procedure. *Netherlands Heart Journal* **25**(2), 125–130 (2017). <https://doi.org/10.1007/s12471-016-0930-7>
- [20] Pozzoli, A., Zuber, M., Reisman, M., Maisano, F., Taramasso, M.: Comparative Anatomy of Mitral and Tricuspid Valve: What Can the

- 1059 Interventionist Learn From the Surgeon. *Frontiers in Cardiovascular*
1060 *Medicine* **5**, 80 (2018). <https://doi.org/10.3389/fcvm.2018.00080>
1061
1062
- 1063 [21] Turton, E.W., Ender, J.: Role of 3D Echocardiography in Cardiac Surgery:
1064 Strengths and Limitations. *Current Anesthesiology Reports* 2017 7:3 **7**(3),
1065 291–298 (2017). <https://doi.org/10.1007/S40140-017-0226-5>
1066
1067
- 1068 [22] Alkhouli, M., Hijazi, Z.M., Holmes, D.R., Rihal, C.S., Wieggers, S.E.:
1069 Intracardiac Echocardiography in Structural Heart Disease Interventions.
1070 *JACC: Cardiovascular Interventions* **11**(21), 2133–2147 (2018). <https://doi.org/10.1016/J.JCIN.2018.06.056>
1071
1072
1073
1074
1075
- 1076 [23] Basman, C., Parmar, Y.J., Kronzon, I.: Why ICE - Intracardiac Echocar-
1077 diography for Structural Heart and Electrophysiological Interventions.
1078 *Current Cardiology Reports* **19**(10) (2017). [https://doi.org/10.1007/](https://doi.org/10.1007/s11886-017-0902-6)
1079 [s11886-017-0902-6](https://doi.org/10.1007/s11886-017-0902-6)
1080
1081
1082
- 1083 [24] Enriquez, A., Saenz, L.C., Rosso, R., Silvestry, F.E., Callans, D., March-
1084 linski, F.E., Garcia, F.: Use of Intracardiac Echocardiography in Inter-
1085 ventional Cardiology. *Circulation* **137**(21), 2278–2294 (2018). [https://doi.](https://doi.org/10.1161/CIRCULATIONAHA.117.031343)
1086 [org/10.1161/CIRCULATIONAHA.117.031343](https://doi.org/10.1161/CIRCULATIONAHA.117.031343)
1087
1088
- 1089 [25] Ancona, F., Stella, S., Taramasso, M., Marini, C., Latib, A., Denti,
1090 P., Grigioni, F., Enriquez-Sarano, M., Alfieri, O., Colombo, A.,
1091 Maisano, F., Agricola, E.: Multimodality imaging of the tricuspid valve
1092 with implication for percutaneous repair approaches. *Heart (British*
1093 *Cardiac Society)* **103**(14), 1073–1081 (2017). [https://doi.org/10.1136/](https://doi.org/10.1136/heartjnl-2016-310939)
1094 [heartjnl-2016-310939](https://doi.org/10.1136/heartjnl-2016-310939)
1095
1096
1097
1098
1099
- 1100 [26] Latib, A., Mangieri, A., Vicentini, L., Ferri, L., Montorfano, M., Ismeno,
1101
1102
1103
1104

- G., Regazzoli, D., Ancona, M.B., Giglio, M., Denti, P., Colombo, A., Agricola, E.: Percutaneous Tricuspid Valve Annuloplasty Under Conscious Sedation (With Only Fluoroscopic and Intracardiac Echocardiography Monitoring). *JACC: Cardiovascular Interventions* **10**(6), 620–621 (2017). <https://doi.org/10.1016/J.JCIN.2016.12.283>
- [27] Pozzoli, A., Taramasso, M., Zuber, M., Maisano, F.: Transcatheter tricuspid valve repair with the MitraClip system using intracardiac echocardiography: Proof of concept. *EuroPCR* (2017). <https://doi.org/10.4244/EIJ-D-17-00360>
- [28] Saji, M., Ailawadi, G., Izarnotegui, V., Fowler, D.E., Lim, D.S.: Intracardiac echocardiography during transcatheter tricuspid valve-in-valve implantation. *Cardiovascular Intervention and Therapeutics* 2017 **33**:3 **33**(3), 285–287 (2017). <https://doi.org/10.1007/S12928-017-0469-6>
- [29] Møller, J.E., De Backer, O., Nuyens, P., Vanhaverbeke, M., Vejlstrup, N., Søndergaard, L.: Transesophageal and intracardiac echocardiography to guide transcatheter tricuspid valve repair with the TriClip™ system. *The International Journal of Cardiovascular Imaging* 2021, 1–3 (2021). <https://doi.org/10.1007/S10554-021-02448-0>
- [30] Fam, N.P., Samargandy, S., Gandhi, S., Eckstein, J.: Intracardiac echocardiography for guidance of transcatheter tricuspid edge-to-edge repair. *EuroIntervention* **14**(9), 1004–1005 (2018). <https://doi.org/10.4244/EIJ-D-18-00672>
- [31] Peters, T.M., Linte, C.A., Yaniv, Z., Williams, J.: *Mixed and Augmented Reality in Medicine*. CRC Press (2018). <https://doi.org/10.1201/9781315157702>

- 1151 [32] Jin, Y., Zhang, Q., liang Mao, J., He, B.: Image-guided left ventricular lead
1152 placement in cardiac resynchronization therapy for patients with heart
1153 failure: A meta-analysis. *BMC Cardiovascular Disorders* **15**(1) (2015).
1154 <https://doi.org/10.1186/s12872-015-0034-0>
1155
1156
1157
- 1158 [33] Overtchouk, P., Delhayé, C., Sudre, A., Modine, T.: Successful tran-
1159 scatheter aortic valve implantation for severe aortic stenosis of a bicuspid
1160 valve with situs inversus totalis guided by advanced image processing: A
1161 case report. *European Heart Journal - Case Reports* **2**(2), 1–4 (2018).
1162 <https://doi.org/10.1093/ehjcr/yty049>
1163
1164
1165
1166
- 1167 [34] Chauhan, K., Dewal, M., Rohit, M.: Automatic detection of vena con-
1168 tracta width for the mitral regurgitation assessment. *International Journal*
1169 *of Computer Science and Management Research* **2**, 2455–2460 (2013)
1170
1171
1172
- 1173 [35] Wang, Y., Vitanovski, D., Georgescu, B., Ionasec, R., Voigt, I., Datta,
1174 S., Gruner, C., Herzog, B., Biaggi, P., Funka-Lea, G., Comaniciu, D.:
1175 Automatic detection and quantification of mitral regurgitation on TTE
1176 with application to assist mitral clip planning and evaluation. *Lecture*
1177 *Notes in Computer Science (including subseries Lecture Notes in Artificial*
1178 *Intelligence and Lecture Notes in Bioinformatics)* **7761 LNCS**, 33–41
1179 (2013). https://doi.org/10.1007/978-3-642-38079-2_5
1180
1181
1182
1183
1184
1185
- 1186 [36] Sotaquirá, M., Pepi, M., Tamborini, G., Caiani, E.G.: Anatomical Regur-
1187 gitant Orifice Detection and Quantification from 3-D Echocardiographic
1188 Images. *Ultrasound in Medicine and Biology* **43**(5), 1048–1057 (2017).
1189 <https://doi.org/10.1016/j.ultrasmedbio.2016.12.017>
1190
1191
1192
- 1193 [37] Li, F.P., Rajchl, M., Moore, J., Peters, T.M.: A mitral annulus track-
1194 ing approach for navigation of off-pump beating heart mitral valve
1195
1196

- repair. *Medical Physics* **42**(1), 456–468 (2015). <https://doi.org/10.1118/1.4904022> 1197
1198
1199
1200
- [38] Courtney, B., Witcomb, N.: Data display and processing algorithms for 3D imaging systems. US Patent (2014) 1201
1202
1203
1204
- [39] Boone, N., Nam, H.H., Moore, J., Carnahan, P., Ginty, O., Herz, C., Lasso, A., Jolley, M.A., Chen, E.C.S., Peters, T.: Patient-specific, dynamic models of hypoplastic left heart syndrome tricuspid valves for simulation and planning. *SPIE*. In: Fei, B., Linte, C.A. (eds.) *Medical Imaging 2020: Image-Guided Procedures, Robotic Interventions, and Modeling*, vol. 11315, pp. 613–621 (2020). <https://doi.org/10.1117/12.2549745> 1205
1206
1207
1208
1209
1210
1211
1212
1213
1214
1215
- [40] Chen, E.C.S., Peters, T.M., Ma, B.: Guided ultrasound calibration: where, how, and how many calibration fiducials. *International Journal of Computer Assisted Radiology and Surgery* **11**(6), 889–898 (2016). <https://doi.org/10.1007/s11548-016-1390-7> 1216
1217
1218
1219
1220
1221
1222
- [41] Nisar, H., Moore, J., Alves-Kotzev, N., Hwang, G.Y.S., Peters, T.M., Chen, E.C.S.: Ultrasound calibration for unique 2.5D conical images. *SPIE*. . In: Fei, B., Linte, C.A. (eds.) *Medical Imaging 2019: Image-Guided Procedures, Robotic Interventions, and Modeling*, p. 78. (2019). <https://doi.org/10.1117/12.2506193> 1223
1224
1225
1226
1227
1228
1229
1230
1231
- [42] Linte, C.A., Moore, J., Peters, T.M.: How accurate is accurate enough? A brief overview on accuracy considerations in image-guided cardiac interventions. *IEEE*. In: 2010 Annual International Conference of the IEEE Engineering in Medicine and Biology, pp. 2313–2316 (2010). <https://doi.org/10.1109/IEMBS.2010.5627652> 1232
1233
1234
1235
1236
1237
1238
1239
1240
1241
1242

- 1243 [43] Singh, S.M., Heist, E.K., Donaldson, D.M., Collins, R.M., Chevalier, J.,
1244 Mela, T., Ruskin, J.N., Mansour, M.C.: Image integration using intrac-
1245 ardiac ultrasound to guide catheter ablation of atrial fibrillation. *Heart*
1246 *Rhythm* **5**(11), 1548–1555 (2008). [https://doi.org/10.1016/j.hrthm.2008.](https://doi.org/10.1016/j.hrthm.2008.08.027)
1247 [08.027](https://doi.org/10.1016/j.hrthm.2008.08.027)
1248
1249
1250
1251
1252
1253
1254
1255
1256
1257
1258
1259
1260
1261
1262
1263
1264
1265
1266
1267
1268
1269
1270
1271
1272
1273
1274
1275
1276
1277
1278
1279
1280
1281
1282
1283
1284
1285
1286
1287
1288